

Natural Language Supervision for Low-light Image Enhancement

Jiahui Tang, Kaihua Zhou, Zhijian Luo and Yueen Hou
School of Computer, Jiaying University, Meizhou, R. P. China, 514015

Abstract—With the development of deep learning, numerous methods for low-light image enhancement (LLIE) have demonstrated remarkable performance. Mainstream LLIE methods typically learn an end-to-end mapping based on pairs of low-light and normal-light images. However, normal-light images under varying illumination conditions serve as reference images, making it difficult to define a “perfect” reference image. This leads to the challenge of reconciling metric-oriented and visual-friendly results. Recently, many cross-modal studies have found that side information from other related modalities can guide visual representation learning. Based on this, we introduce a Natural Language Supervision (NLS) strategy, which learns feature maps from text corresponding to images, offering a general and flexible interface for describing an image under different illumination.

However, image distributions conditioned on textual descriptions are highly multimodal, which makes training difficult. To address this issue, we design a Textual Guidance Conditioning Mechanism (TCM) that incorporates the connections between image regions and sentence words, enhancing the ability to capture fine-grained cross-modal cues for images and text. This strategy not only utilizes a wider range of supervised sources, but also provides a new paradigm for LLIE based on visual and textual feature alignment. In order to effectively identify and merge features from various levels of image and textual information, we design an Information Fusion Attention (IFA) module to enhance different regions at different levels. We integrate the proposed TCM and IFA into a Natural Language Supervision network for LLIE, named NaLSuper. Finally, extensive experiments demonstrate the robustness and superior effectiveness of our proposed NaLSuper.

Index Terms—Low-light image enhancement; Natural language supervision; attention mechanism.

I. INTRODUCTION

HIGH-QUALITY images are crucial for various advanced computer vision tasks, e.g., object detection[30], image classification[1] and semantic segmentation[16], etc. However, images captured in low-light conditions often suffer from issues like low contrast, low brightness, and serious noises. Therefore, it is practically important to address brightness degradation to facilitate the exploration of sophisticated dark environments. To improve the quality of these images, numerous low-light image enhancement (LLIE) methods[33], [8], [10], [13], [31], [12], [19], [54] have been proposed in recent years.

In recent years, the effectiveness of deep learning methods in computer vision applications has spurred their application in LLIE[37], [12] [50], [31], [26], [42], [53], [62]. These deep learning-based methods for LLIE can be categorized into two main groups: Retinex-based methods[50], [29], [32], and end-to-end methods[27], [19]. Retinex-based methods initially

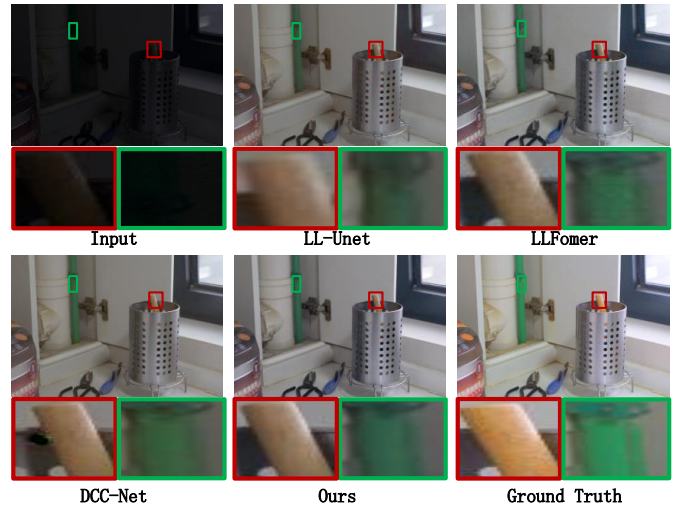


Fig. 1. Comparison with state-of-the-art methods on LOLv1 dataset. It is evident that we have restored more authentic colors and visually appealing content.

decompose the image into illumination and reflectance component using a convolutional neural network. These components are then processed separately before being recombined to produce the final enhanced image. However, Retinex-based models are prone to image stylization and noise amplification due to inadequate decomposition of reflectance and illumination, which leads to optimization challenges. On the other hand, end-to-end methods aim to learn the mapping between low-light and normal-light images without relying on any physical model. Despite their potential, current end-to-end methods face issues such as underexposure, overexposure, and color imbalance, and their overall generalization performance remains relatively low.

The goal of LLIE is ensuring that the enhanced image’s subjective visual experience closely resembles that of a natural image under normal lighting. To achieve this, many existing methods mainly use normal-light image as a supervisory constraint. However, the variability in illumination of these normal-light images makes it difficult to define a “perfect” reference image. Furthermore, existing methods primarily focus on generating results that perform well according to specific metrics, often at the expense of visual quality. Thus these methods face the challenge of reconciling metric-oriented and visual-friendly result.

Recent research in cross-modal learning[35], [45], [7], [63] has shown that side information from related modalities can

effectively guide visual representation learning. Based on this, we propose that learning from text corresponding to images is a promising alternative for LLIE, providing a general and flexible interface for describing an image of different illuminations. Building on this foundation, to enhance low-light image, we propose a Natural Language Supervision strategy, which jointly learns feature maps from text and corresponding image. However, the highly multimodal distribution of images conditioned on textual descriptions poses training challenges, limiting the application of natural language supervision in LLIE. The work[51] found that incorporating the connections between image regions and sentence words generally, which enhances the ability of network to capture fine-grained cross-modal cues for images and text. Building upon this inspiration, we introduce a Textual Guidance Conditioning Mechanism (TCM), employing cross-attention to comprehensively capture both cross-modal and intra-modal relationships between image regions and sentence words.

As the network goes deeper and deeper, shallow feature of text and image information is often difficult to preserve. In order to effectively identify and merge features from various levels of image and textual information, we design a novel information fusion attention (IFA) module to improve feature representation, which can provide additional flexibility in dealing with different modal of information.

In this paper, we propose a Natural Language Supervision network (denoted as NaLSuper) for LLIE, which incorporates TCM and IFA modules. Overall, our contributions can be summarized as follows:

- 1) We propose a Natural Language Supervision network (denoted as NaLSuper) for LLIE, which incorporates Textual Guidance Conditioning Mechanism (TCM) and Information Fusion Attention (IFA) modules.
- 2) We are the first to utilize a Natural Language Supervision strategy in LLIE, which use this strategy results in better visual effect of the enhanced image. To address the training challenges posed by this strategy in a multi-modal data distribution, we have developed the TCM, which can comprehensively capture both cross-modal and intra-modal relationships between image regions and sentence words.
- 3) We design a novel information fusion attention (IFA) module to improve feature representation, which can provide additional flexibility in dealing with different modal of information. Thanks to this module, our network can effectively identify and merge features from various levels of image and textual information.
- 4) Extensive tests conducted on four benchmark dataset reveal that the proposed NaLSuper outperforms recent state-of-the-art methods in both quantitative and qualitative evaluations of quality.

II. RELATED WORK

A. Low-light Image Enhancement

1) *Traditional Cognition Methods*: In regions with low lighting, pixel values are generally lower. It is a very forthright idea to directly adjust brightness of image through enhance

these lower pixel values, which is referred to as value-based. The value-based methods include histogram equalization (HE) and gamma correction (GC). The conventional HE method [4] alters the histogram distribution. While it adjusts the illumination of the image, it introduces issues such as artifacts, loss of detail, overexposure, and color distortion. To address these shortcomings, researchers have implemented a series of enhancements to HE. Kim *et al.*[23] introduced Brightness Bihistogram Equalization (BBEH), while Wang *et al.* [47] proposed Dualistic Subimage Histogram Equalization (DSHE), both of which aimed to produce more natural-looking equalized images. Nonetheless, the visual artifacts in images equalized by HE methods remain their primary drawback.

GC employs nonlinear transformations to enhance the gray values in darker areas of the image while reducing the gray values in areas with excessively high gray values. Traditional gamma transformations used for low-light image enhancement suffer from clear drawbacks, including unnatural images, uneven exposure, and loss of details. To address these issues, Bennett *et al.*[2] enhanced image brightness using Per-Pixel Virtual Exposures. However, the GC method still suffers from uneven exposure.

2) *Deep Learning Methods*: With the successful application of deep learning in computer vision [40] and image processing [24], researchers have turned to deep learning techniques for LLIE. For instance, Lore *et al.* [31] introduced LLNet, a stacked sparse denoising auto-encoder designed for simultaneous low-light enhancement and noise reduction. Wei *et al.* [50] introduced a CNN-based Retinex decomposition method, establishing a deep network that integrates image decomposition and subsequent enhancement operations. Zhang *et al.* [60] merged Retinex theory with convolutional neural networks, dividing the network into two parts: illumination and reflectance estimation, and training it using gamma-corrected simulation data. Subsequently, Zhang *et al.* [59] optimized the model structure based on KinD, resulting in KinD++. Hao *et al.* [14] achieved Retinex image decomposition in a semi-decoupled manner. Liu *et al.* [29] proposed a lightweight method called Retinex-inspired Unrolling with Architecture Search (RUAS) for efficient low-light image enhancement. Ma *et al.* [32] summarized deep learning methods based on Retinex theory and a context-sensitive decomposition network, along with supervised and self-supervised versions. Zhu *et al.* [65] proposed a method involving a learnable guidance map from signal and deep priors, enabling adaptive enhancement of low-light images in a region-dependent manner. Zhao *et al.* [62] introduced a Retinex decomposition "generative" strategy, which formed the basis for a unified deep framework to estimate latent components and enhance low-light images. Wu *et al.* [52] developed three neural modules that facilitate image recovery in three phases: initialization, optimization, and illumination adjustment. The previous methods aimed at LLIE were either designed within a single scale framework or implemented through a cascaded process, which limits their effectiveness across various low-light conditions.

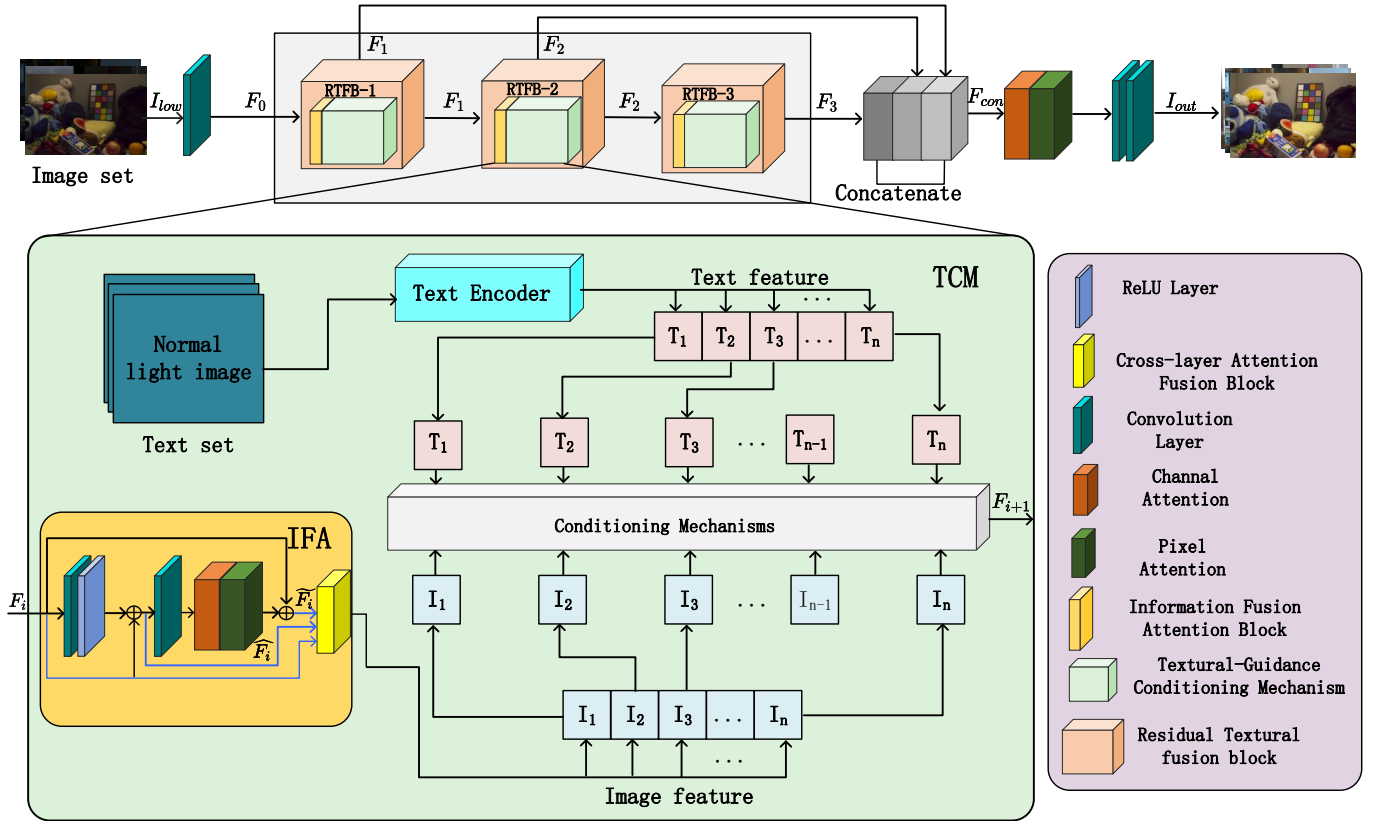


Fig. 2. Overview architecture of our proposed NaLSuper. NaLSuper is a Natural Language Supervision network for LLIE, which incorporates Textual Guidance Conditioning Mechanism (TCM) and Information Fusion Attention (IFA) modules. The final estimation outputted by the reconstruction part and global residual learning structure, which is considered to be the desired normal-light image.

B. Natural Language Supervision

Vision-language pretraining has recently emerged as a promising approach for understanding images [18], [35], [45] and videos [43]. Unlike traditional approaches that rely on discrete labels, it introduces a new recognition paradigm based on the alignment of visual and textual features. Recent studies have also explored how to utilize the transferable knowledge of pre-trained models for tasks such as visual question answering (VQA) [20], zero-shot object detection [11], and image captioning [38]. For example, Radford et al. [35] introduced CLIP, a method for learning visual models under language supervision. After being trained on 400 million image-text pairs, CLIP is capable of describing any visual concept in natural language and can be applied to other tasks without further specific training. Zhou et al. [64] introduced soft prompts, utilizing learnable vectors to model context words instead of traditional hand-crafted prompts, thereby capturing task-relevant context. Rao et al. [36] innovatively introduced context-aware prompting, integrating prompts with visual features for more precise instance-level refinement. Cho et al. [5] harmonized prior knowledge across various tasks through a unified framework tailored to seven multi-modal tasks. Additionally, Ju et al. [22] leveraged the pre-trained CLIP model to enhance video comprehension. In this paper, we aim to explore how natural language supervision can be utilized for LLIE.

III. METHOD

In this section, we mainly introduce a Natural Language Supervision network (denoted as NaLSuper) for LLIE. As illustrated in Fig. 2, the input of NaLSuper is a low light image $I_{low} \in \mathbb{R}^{H \times W \times 3}$, it is first passed into a 3×3 convolution as a projection layer to extract shallow feature $F_0 \in \mathbb{R}^{H \times W \times C}$. Next, F_0 is fed into three Residual Textual guide Fusion Block (RTFB) with multiple skip connections, which can extract deeper feature of fine-grained cross-modal information for images and text. Specifically, intermediate features outputted from RTFB are denoted as $F_1, F_2, F_3 \in \mathbb{R}^{H \times W \times C}$. After that, these features F_1, F_2, F_3 will be concatenate to $F_{con} \in \mathbb{R}^{H \times W \times 3C}$, and then it passed to the reconstruction part and global residual learning structure, thereby getting a enhanced image $I_{out} \in \mathbb{R}^{H \times W \times 3}$.

Furthermore, we combines RTFB Architecture with local residual learning, every RTFB combines the Textual Guidance Conditioning Mechanism (TCM) and Information Fusion Attention (IFA) modules.

A. Textual Guidance Conditioning Mechanism (TCM)

Current approaches predominantly rely on image-level supervision, where the output is constrained to closely resemble target images. Yet, these methods faces challenges due to significant brightness discrepancies among different

references, which can complicate model training. Additionally, some references exhibit visual flaws, such as unnatural brightness, resulting in outputs that are visually unappealing. To alleviate training complexities and reconcile the disparity between metric-oriented and visually pleasing versions, as shown in Fig. 2, we design a Textual Guidance Conditioning Mechanism (TCM) to comprehensively capture both cross-modal and intra-modal relationships between image regions and sentence words.

1) *Text Encoder*: The main objective of the text encoder is to map the raw textual descriptions of interactions to the feature space. The raw text will be broken down into tokens and transformed into a series of word embeddings. Recent research [35], [64] indicates that the selection of context words around the class name can greatly affect the accuracy of recognition. In this work, we employ the recent well-known pretrained CLIP[35] text encoder and keep it fixed during training. As shown in Fig. 2, We first manually design a series of prompt, such as normal light image. After CLIP, text feature $T_i, [i = 1, 2, \dots, n]$ is obtained, which has textual semantic information of corresponding image.

2) *Conditioning Mechanisms*: Image distributions conditioned on textual descriptions are highly multimodal, which makes training difficult. To address this problem, we use the cross-attention mechanism as the fusion layer (refer to Fig. 2), which is valid for attention-based models that learn relationships between various input modalities [17]. To preprocess T_i from different modalities (such as language prompts), we utilize a domain-specific encoder τ_θ that maps T_i to an intermediate representation $\tau_\theta(T_i)$ in $\mathbb{R}^{d_\tau \times M}$. Then the computation of query matrix Q , key matrix K , and value matrix V are as follow:

$$Q = W_q \cdot \psi(I_i), K = W_k \cdot \tau_\theta(T_i), V = W_v \cdot \tau_\theta(T_i), \quad (1)$$

where $W_q \in \mathbb{R}^{d \times d_\zeta}$, $W_k \in \mathbb{R}^{d \times d_\tau}$, and $W_v \in \mathbb{R}^{d \times d_\tau}$ represent the projection matrices[17], [41], $I_i, [i = 1, 2, \dots, n]$ represent a feature map of image and $\psi(I_i) \in \mathbb{R}^{d_\zeta \times M}$ denotes a (flattened) intermediate representation. Suppose that we have $Q, K, V \in \mathbb{R}^{d \times M}$, and the attention matrix is expressed as:

$$\text{Attention}(Q, K, V) = \text{softmax} \left(\frac{QK^T}{\sqrt{d}} + B \right) V, \quad (2)$$

where B is a learnable matrix of relative position encoding. Refer to Fig. 2 for a visual representation.

B. Information Fusion Attention (IFA)

Many LLIE networks uniformly process channel-wise and pixel-wise features, which fails to effectively address images with uneven illumination distribution and weighted channel-wise features. Additionally, the network goes deeper and deeper, shallow feature of text and image information is often difficult to preserve. In order to effectively identify and merge features from various levels of image and textual information. We design a Information Fusion Attention (IFA) module (refer to Fig. 3) includes both channel attention, pixel attention and Cross-layer Attention Fusion Block, which can provide additional flexibility in dealing with different modal of information.

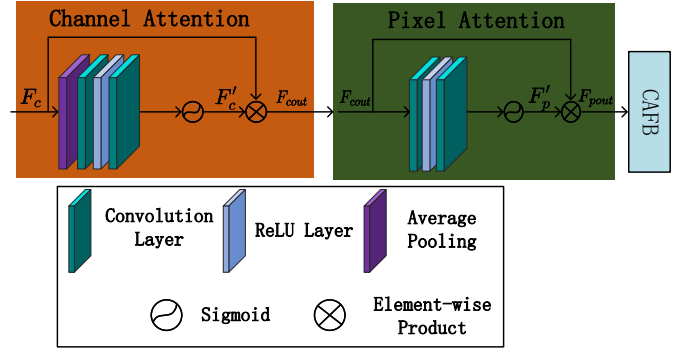


Fig. 3. Overview architecture of Information Fusion Attention (IFA).

1) *Channel Attention*: Our channel attention focuses on the concept that various channel features carry distinctly different weights of information in relation to DCP [15]. Inspired by [34], we capture the channel-wise global spatial information through a channel descriptor by employing global average pooling.

$$g_c = P(F_c) = \frac{1}{H \times W} \sum_{i=1}^H \sum_{j=1}^W X_c(i, j) \quad (3)$$

Eq. 3 represents the global average pooling operation $P(\cdot)$ applied to a feature map. g_c is the pooled feature for the channel c , obtained by averaging all pixel values $X_c(i, j)$ across the spatial dimensions H (height) and W (width) of the feature map F_c . This reduces the spatial dimensions of each channel to 1×1 , effectively compressing the spatial information of the feature map into a single value per channel.

To determine the weights of various channels, the features go through two convolutional layers and subsequently are activated using sigmoid and ReLU functions. Finally, an element-wise multiplication is performed between the input feature map F_c and the channel-specific weights. The Channel Attention process is formulated as:

$$F'_c = \text{Sigmoid}(\text{Conv}(\text{ReLU}(\text{Conv}(g_c)))), \quad (4)$$

$$F_{cout} = CA(F_c) = F'_c \otimes F_c.$$

2) *Pixel Attention*: Given the uneven distribution of illumination across different pixels in an image, we employ a pixel attention module to make the network pay more attention to informative features. This includes areas with low-light and regions of the image with high frequency.

Similar to [34], we directly feed the input F_{cout} into two convolutional layers and subsequently are activated using sigmoid and ReLU functions. Finally, an element-wise multiplication is performed between the input feature map F_{cout} and the pixel-specific weights. The Pixel Attention process is formulated as:

$$F'_p = \text{Sigmoid}(\text{Conv}(\text{ReLU}(\text{Conv}(F_{cout})))), \quad (5)$$

$$F_{pout} = CA(F_c) = F'_p \otimes F_{cout}.$$

3) *Cross-layer Attention Fusion Block*: Recent methods using transformers incorporate feature connections or skip connections to merge features across various layers, as discussed

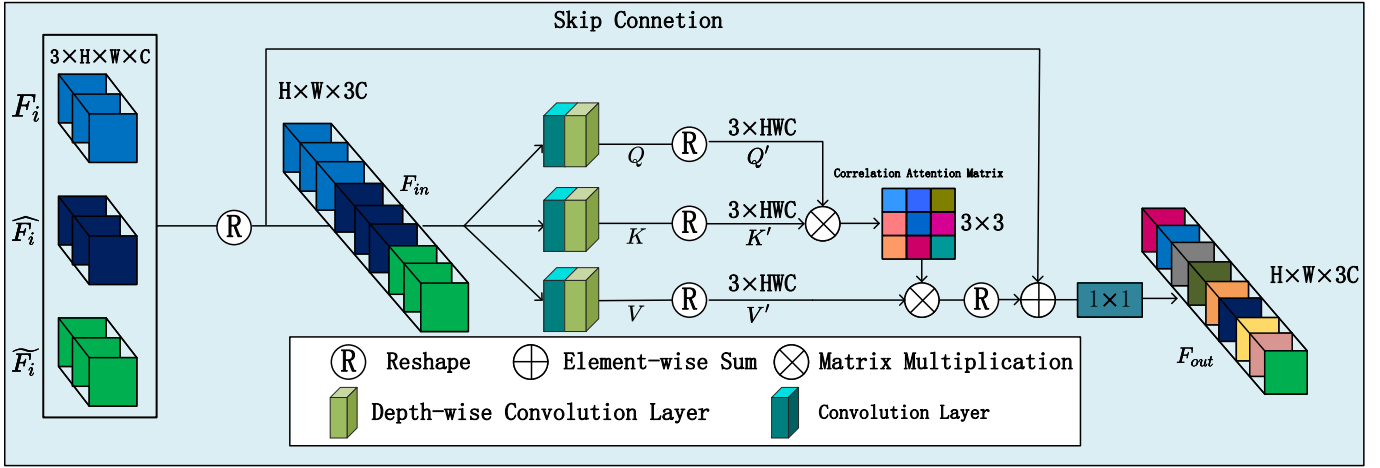


Fig. 4. Overview architecture of Cross-layer Attention Fusion Block(CAFB).

in studies by Zamir et al. [57] and Wang et al. [48]. Nevertheless, these methods do not completely leverage the inter-layer dependencies, which restricts their ability to represent complex features effectively. To address this problem, we use a Cross-layer Attention Fusion Block(CAFB) [46], which adaptively fuses hierarchical features with learnable correlations among different layers. The underlying concept of CAFB is that activations in various layers correspond to specific classes, and the correlations between these features can be dynamically learned through a self-attention mechanism.

As show in Fig. 2, given features $F_i, \hat{F}_i, \tilde{F}_i \in \mathbb{R}^{H \times W \times C}$, we concatenate and reshape them to make $F_{in} \in \mathbb{R}^{H \times W \times 3C}$. Following [46], we use 1×1 convolutional layers to integrate context across different channels at the pixel level, and then apply 3×3 depth-wise convolutions to generate Q, K , and V . We reshape the matrices Q and K into 2D forms with dimensions $3 \times HWC$ (denoted as Q') and $3 \times HWC$ (denoted as K'), respectively. This restructuring allows us to compute the layer correlation attention matrix A , which has a size of 3×3 . Finally, we scale the reshaped value $V' \in \mathbb{R}^{HWC \times 3}$ by multiplying it with the attention matrix A and a scaling factor δ .

$$\text{Cross-Layer}(Q', K', V') = \text{softmax}\left(\frac{Q'K'}{\delta}\right) V', \quad (6)$$

Then, we add the input features F_{in} to this product. The CAFB process is formulated as:

$$F_{out} = \text{Cross-Layer}(Q', K', V') + F_{in}, \quad (7)$$

F_{out} represents the output feature that targets the informative layers within the network. In practical terms, we strategically position the CAFB at locations in the tail of each RTFB. This placement enables CAFB to effectively capture long-distance dependencies across hierarchical layers during both the feature extraction and image reconstruction phases.

C. Loss Function

There are two reconstruction loss terms to train our framework, i.e., the L_1 loss and the SSIM loss. The L_1 loss is

written as

$$L_1 = \frac{1}{n} \sum_{i=1}^n \|I_{gt}^i - \text{enhanced}(I_{low}^i)\|, \quad (8)$$

where I_{gt} denotes the ground truth, n is the batch size and I_{low} stands for input(low-light image). The SSIM loss is written as

$$L_{SSIM} = \frac{1}{n} \sum_{i=1}^n \left(\frac{(2\mu_{I_{gt}}^i \cdot \mu_{I_{low}}^i + c_1) \cdot (2\sigma_{I_{gt}^i, I_{low}^i} + c_2)}{(\mu_{I_{gt}}^2 + \mu_{I_{low}}^2 + c_1) \cdot (\sigma_{I_{gt}}^2 + \sigma_{I_{low}}^2 + c_2)} \right), \quad (9)$$

where μ is the variances, and σ is the covariance. c_1 and c_2 are constants added to avoid having a denominator of zero. The overall loss function is

$$L = L_1 + L_{SSIM}. \quad (10)$$

IV. EXPERIMENTAL RESULTS

A. Benchmark Datasets

To evolution the performance and efficiency of the proposed NaLSuper, we test our approach on several publicly accessible low-light datasets, such as LOLv1 [50], LOLv2, [55] and SID [3].

The LOL dataset is available in two versions: v1 and v2. LOLv1 provides 485 pairs of low-/normal-light images for training and 15 pairs for testing. Each pair consists of a low-light image and its corresponding well-exposed reference image. LOLv2 is split into two subsets: LOLv2-real and LOLv2-synthetic. The training set for LOLv2-real includes 689 pairs of low-/normal-light images, and the test set comprises 100 pairs. These low-light images are primarily captured in various settings by adjusting the ISO and exposure time, while keeping other parameters constant. LOL-v2-synthetic, however, is generated by analyzing the light distribution in low-light images and then synthesizing these from RAW images.

The subset of the SID dataset captured with the Sony $\alpha 7S$ II camera is used for evaluation. It comprises 2697 pairs of short/long-exposure RAW images. The low-/normal-light RGB images are derived by applying the same in-camera signal processing used in SID to convert the RAW images into the



Fig. 5. Visual comparison with LLIE methods on LOLv1 dataset.

RGB format. Specifically, 2099 image pairs are utilized for training, while 598 pairs are designated for testing.

The four widely adopted quality metrics, i.e., peak signal-to-noise ratio (PSNR), structural similarity (SSIM)[49], LPIPS and mean absolute error (MAE), are adopted for quantitative comparison as evaluation metrics between the enhanced images and the referenced ground truths. For the metrics PSNR and SSIM, higher values signify improved image quality. Conversely, a lower LPIPS and MAE score indicates superior quality.

B. Implementation Details

For model training of our proposed network, we use the Adam optimizer with a learning rate of 10^{-4} . All experiments on benchmark datasets are implemented with PyTorch, on a 64 core Intel Xeon Gold 6226R CPU @2.90GHz, 256 GB memory and a Nvidia Quadro RTX 8000 GPU.

C. Quantitative Evaluation

To evaluate the advantages of proposed NaLSuper, we quantitatively compare our proposed method with several

| Methods | LOLv1 | | | |
|-----------------|-----------------|-----------------|--------------------|------------------|
| | PSNR \uparrow | SSIM \uparrow | LPIPS \downarrow | MAE \downarrow |
| BIMEF [56] | 13.88 | 0.595 | 0.3264 | 0.2063 |
| FEA [6] | 16.72 | 0.478 | 0.3847 | 0.1421 |
| LIME [13] | 16.76 | 0.445 | 0.3945 | 0.1200 |
| MF [9] | 16.97 | 0.508 | 0.3796 | 0.1416 |
| NPE [44] | 16.97 | 0.484 | 0.4049 | 0.1290 |
| SRIE [10] | 11.86 | 0.495 | 0.3401 | 0.2571 |
| MSRCR [21] | 13.17 | 0.462 | 0.4350 | 0.2067 |
| RetinexNet [50] | 16.77 | 0.425 | 0.4739 | 0.1256 |
| DSLRL [28] | 14.98 | 0.596 | 0.3757 | 0.1918 |
| KinD [60] | 17.65 | 0.772 | 0.1750 | 0.1231 |
| Z_DCE [12] | 14.86 | 0.562 | 0.3352 | 0.1846 |
| Z_DCE++ [25] | 14.75 | 0.518 | 0.3284 | 0.1801 |
| MIRNet [58] | 20.34 | 0.786 | 0.1688 | 0.1123 |
| RUAS [29] | 16.40 | 0.503 | 0.2701 | 0.1534 |
| ELGAN [19] | 17.48 | 0.652 | 0.3223 | 0.1352 |
| Uformer [48] | 18.55 | 0.721 | 0.3205 | 0.113 |
| Restormer [57] | 22.37 | 0.816 | 0.1413 | 0.0721 |
| LL-Unet[39] | 21.46 | 0.789 | 0.2077 | 0.2630 |
| DDC-net [61] | 22.98 | 0.851 | 0.0905 | 0.0856 |
| LLFormer [46] | 23.65 | 0.816 | 0.1692 | 0.0754 |
| NaLSuper | 24.01 | 0.863 | 0.0747 | 0.0756 |

TABLE I
COMPARISON OF AVERAGE PSNR/SSIM/LPIPS/MAE ON LOLV1 TEST DATASET. THE BEST RESULTS ARE MARKED IN RED COLOR AND THE SECOND BEST RESULTS ARE MARKED IN BLUE COLOR.



Fig. 6. Visual comparison with LLIE methods on LOLv1 dataset.

| Methods | LOLv2-real | | LOLv2-syn | | SID | |
|-----------------|-----------------|-----------------|-----------------|-----------------|-----------------|-----------------|
| | PSNR \uparrow | SSIM \uparrow | PSNR \uparrow | SSIM \uparrow | PSNR \uparrow | SSIM \uparrow |
| KinD [60] | 17.54 | 0.669 | 13.29 | 0.578 | 18.02 | 0.583 |
| RetinexNet [50] | 16.10 | 0.410 | 17.13 | 0.809 | 16.48 | 0.578 |
| ELGAN [19] | 18.64 | 0.670 | 16.57 | 0.737 | 17.23 | 0.543 |
| RUAS [29] | 18.37 | 0.723 | 16.55 | 0.652 | 18.44 | 0.581 |
| Uformer [48] | 18.82 | 0.771 | 19.66 | 0.871 | 18.54 | 0.577 |
| MIRNet [58] | 20.02 | 0.820 | 21.94 | 0.876 | 20.84 | 0.605 |
| Restormer [57] | 19.94 | 0.827 | 21.41 | 0.830 | 22.27 | 0.649 |
| LLformer [46] | 21.73 | 0.819 | 23.24 | 0.894 | — | — |
| NaLSper | 21.12 | 0.840 | 24.48 | 0.929 | 22.22 | 0.610 |

TABLE II

COMPARISON OF AVERAGE PSNR/SSIM ON LOLV2-REAL, LOLV2-SYN AND SID TEST DATASET. THE BEST RESULTS ARE MARKED IN RED COLOR AND THE SECOND BEST RESULTS ARE MARKED IN BLUE COLOR.

LLIE state-of-the-art competitors, including BIMEF [56], FEA [6], LIME [13], MF [9], NPE [44], SRIE [10], MSCRCR [21], RetinexNet [50], DSLR [28], KinD [60], MIRNet [58], Z_DCE [12], Z_DCE++ [25], RUAS [29], ELGAN [19], Uformer [48], Restormer [57], LL-UNet [39], DDC-net [61], LLFormer [46]. We utilize the publicly available source code and recommended parameters for each of the compared methods, and fine-tune all models on the training dataset to enable comparison.

Table I tabulates the comparisons of averaged PSNR/SSIM/LPIPS/MAE scores tested on the LOLv1

testset. The top two results are marked in red, blue. The comparative results presented in the table clearly demonstrate that the proposed NaLSuper significantly outperforms other state-of-the-art methods on the LOLv1 testset. More specifically, our approach achieves the highest PSNR score compared to all other methods and exhibits substantial improvements, with gains reaching up to 0.36dB over the second-best results for the LOLv1 testset. The outstanding performance suggests that our method excels in producing results, which are highly faithful to the ground truths. Additionally, our approach also achieves the best SSIM and



Fig. 7. Visual comparison with LLIE methods on LOLv1 dataset.

LPIPS scores compared to other competitors. Unlike PSNR, the SSIM and LPIPS quality metrics align more closely with the human visual system (HVS), providing a better consistency. As shown in Table I, the SSIM improvements reach up to 0.012 above the second-best results, while the LPIPS improvements reduce to 0.0158 below the second-best results for the LOLv1 test set. Moreover, the MAE scores also achieves the secondly compared to other competitors.

Table II tabulates the comparisons of averaged PSNR/SSIM scores tested on the LOLv2-real, LOL-v2-syn and SID testset. The comparative results presented in the table clearly demonstrate that the proposed NaLSuper significantly outperforms other state-of-the-art methods on the LOLv2-real, LOLv2-syn and SID testset. More specifically, our approach achieves the highest PSNR score compared to all other methods and exhibits substantial improvements, with gains reaching up to $-$ dB, $-$ dB and $-$ dB over the second-best results for the LOLv2-real, LOL-v2-syn and SID testset. The outstanding performance suggests that our method excels in producing results, which are highly faithful to the ground truths. Additionally, our approach also achieves the best SSIM scores compared to other competitors. As shown in Table II, the SSIM

improvements reach up to $-$ above the second-best results for the LOLv2-real, LOL-v2-syn and SID testset. The remarkable results confirm that our method not only delivers the most accurate reconstruction but also excels in performance according to perceptual-oriented assessment outcomes.

D. Subjective Evaluation

To further demonstrate the superiority of the proposed low-light image enhancement method over other competitors, we have selected nine methods with higher PSNR values for comparison on the LOLv1 and LOLv2-real dataset. The visual quality comparison results are shown in Fig. 5–8. The images contained in the LOLv1 and LOLv2-real dataset are taken indoors and are very dark and noisy, which is very challenging for many LLIE methods. The images with the LOLv1 and LOLv2-real dataset are captured indoors, characterized by low light and high noise levels, presenting a significant challenge for numerous LLIE methods. Based on the comparison results, our method demonstrates the most realistic outcomes, exhibiting minimal artifacts and noise in the predominant regions. Moreover, the enhanced results exhibit the most faithful representation of the target image in terms of brightness,

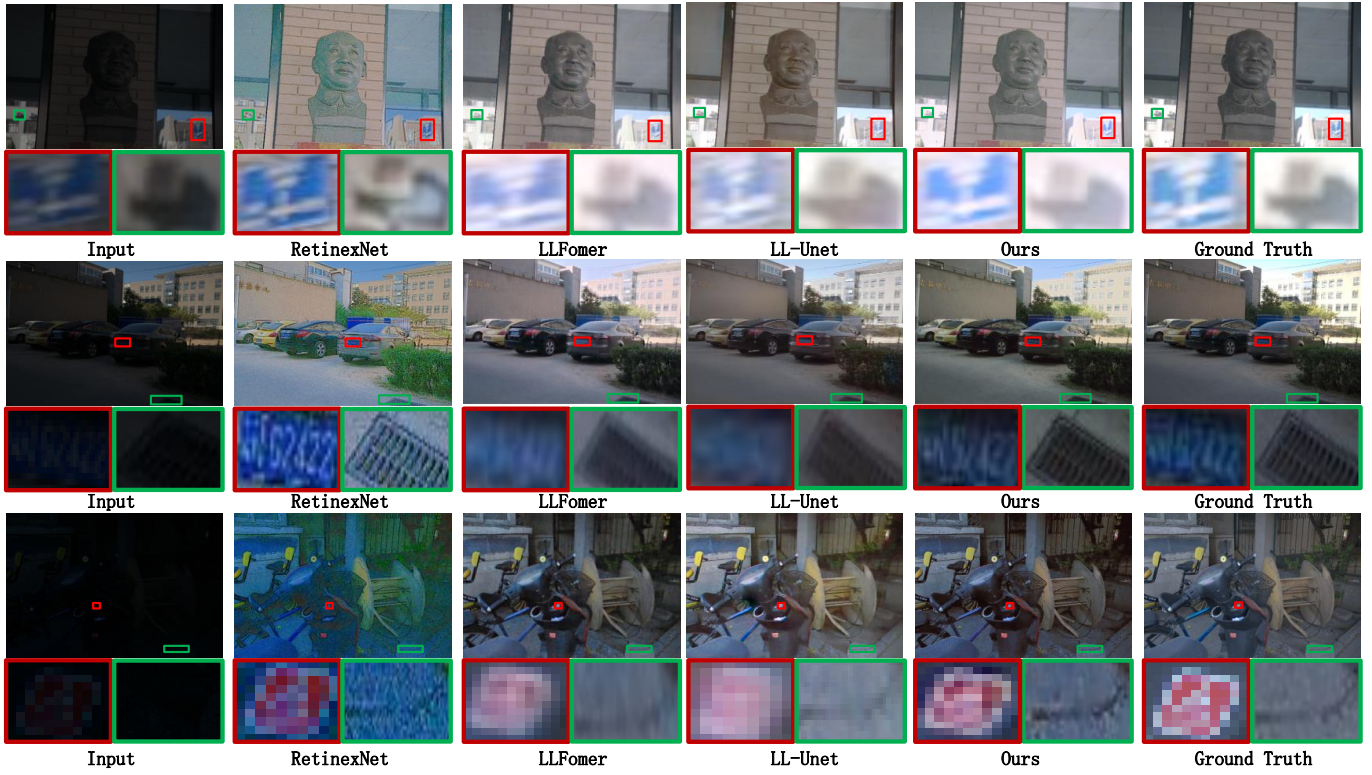


Fig. 8. Visual comparison with LLIE methods on LOLv2-real dataset.

contrast, and color. In comparison, other methods that were evaluated tend to create lots of unexpected halos in edge and textural areas, and some even cause noticeable color distortions across the reconstructed images. The proposed method benefits from the carefully designed natural language supervision strategy, enabling it to effectively address multiple complex degradations in extremely dark environments. It demonstrates proficient restoration of brightness, color, contrast, and detail.

E. Ablation Study

1) *Model Architecture*: To verify the advantages of the network architecture, we conducted an ablation study. We refer to the simplest version of the network, which lacks any specialized modules, as "base". Building on this "base" model, we introduce various configurations to determine if the ultimate model is indeed optimal. These models, each featuring a different configuration, are trained using a consistent strategy and evaluated across three publicly accessible datasets.

Based on the average and standard deviation of PSNR, SSIM, LPIPS, and MAE as presented in Table III, the performance of Base has achieved comparable scores, demonstrating its efficacy. As illustrated in Fig. 9, on the basis of the Base module, integrated IFA can achieving the higher average values but this results in the loss of detail. In comparison, TCM can make them in images cleaner, which makes the image visual better. After combining the TCM and IFA, the result can be more vivid and natural appearance that enhances visual perception. It not only achieves the highest indicators but also has a good visual effect. Harmonization of metric-oriented and visually friendly results is achieved.

| Configuration | Metric | LOLv1 | LOLv2-real | LOLv2-syn |
|---------------|---------|--------|------------|-----------|
| Base | PSNR ↑ | 19.50 | 19.03 | 21.63 |
| | SSIM ↑ | 0.787 | 0.803 | 0.894 |
| | LPIPS ↓ | 0.1697 | 0.2132 | 0.0805 |
| | MAE ↓ | 0.1260 | 0.1376 | 0.0891 |
| +IFA | PSNR ↑ | 20.93 | 20.45 | 24.63 |
| | SSIM ↑ | 0.821 | 0.844 | 0.933 |
| | LPIPS ↓ | 0.1068 | 0.1061 | 0.0385 |
| | MAE ↓ | 0.1082 | 0.1231 | 0.0703 |
| +TCM | PSNR ↑ | 22.33 | 18.71 | 23.39 |
| | SSIM ↑ | 0.830 | 0.818 | 0.922 |
| | LPIPS ↓ | 0.1181 | 0.1227 | 0.0532 |
| | MAE ↓ | 0.0877 | 0.1480 | 0.0751 |
| +IFA+TCM | PSNR ↑ | 24.01 | 21.12 | 24.48 |
| | SSIM ↑ | 0.863 | 0.846 | 0.929 |
| | LPIPS ↓ | 0.0747 | 0.1001 | 0.0396 |
| | MAE ↓ | 0.0756 | 0.1173 | 0.0718 |

TABLE III
THE DETAILED ABLATION ANALYSIS OF EACH COMPONENT UNDER VARIOUS TRAINING CONFIGURATIONS REVEALS THAT THE CONFIGURATION INCORPORATING ALL THE DESIGNED COMPONENTS YIELDS THE BEST RESULTS.

2) *Hyperparameters Experiments*: In the experiment of hyperparameters, we mainly introduce the Residual Textual guide Fusion Block(RTFB) and loss function selected by the model. We configure different numbers of RTFB: 3, 5, 8, 12, 15 and 20. We train models with different numbers of RTFB using the same parameters After comparison in the LOLv1 dataset, the number of 15 achieve the best performance(as shown in Table IV and Fig. 10).

In evaluating different loss functions, we initially selected the basic smooth L1 loss and the recently popular SSIM loss for image processing, before ultimately settling on a combination of SSIM and L1 loss. Experimental results, as detailed in

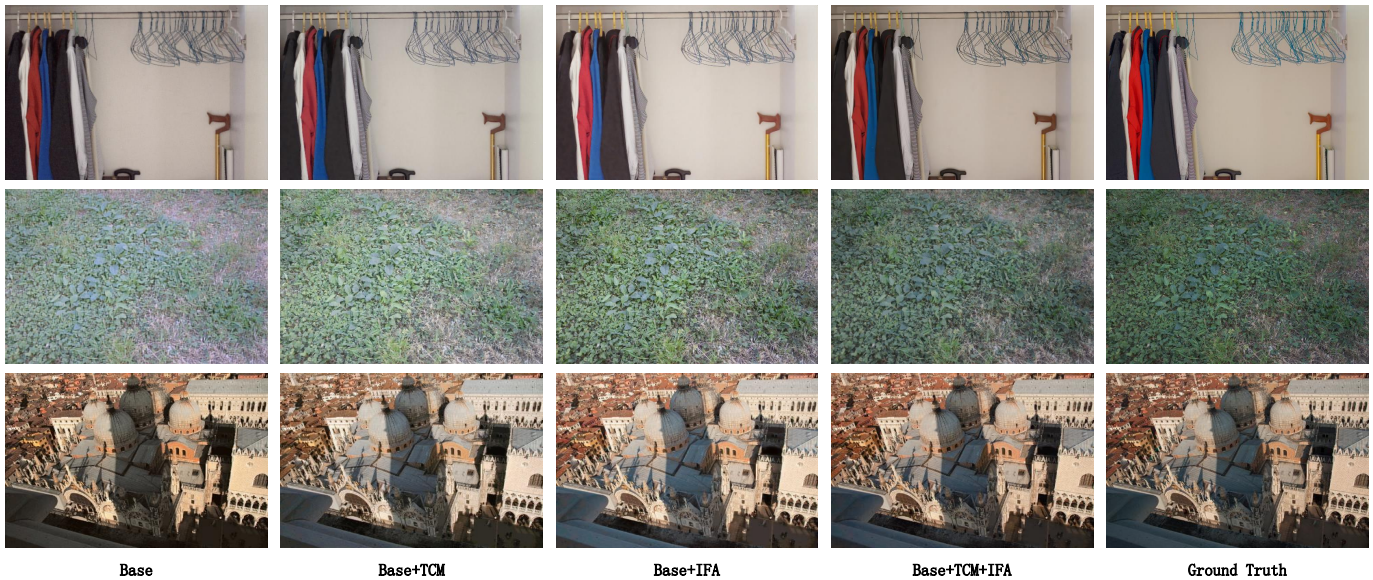


Fig. 9. Comparison of the subjective visual effects of models with varying configurations.

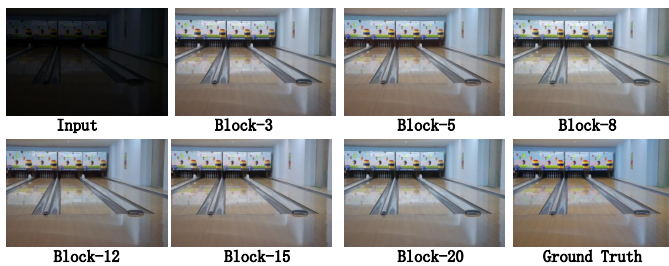


Fig. 10. Comparison of the subjective visual effects of models with different numbers of RTFB .

| Blocks | PSNR \uparrow | SSIM \uparrow | LPIPS \downarrow | MAE \downarrow |
|-----------|-----------------|-----------------|--------------------|------------------|
| 3 | 23.38 | 0.852 | 0.0876 | 0.0767 |
| 5 | 22.49 | 0.845 | 0.0847 | 0.0876 |
| 8 | 23.16 | 0.854 | 0.0863 | 0.0816 |
| 12 | 22.46 | 0.857 | 0.0788 | 0.0862 |
| 15 | 24.01 | 0.863 | 0.0747 | 0.0756 |
| 20 | 23.64 | 0.858 | 0.0773 | 0.0816 |

TABLE IV

PSNR, SSIM, LPIPS, AND MAE EVALUATION OF VARIOUS NUMBERS OF RESIDUAL TEXTUAL GUIDE FUSION BLOCK(RTFB) ON LOLV1 DATASET.

Table V, demonstrate that the SSIM loss effectively enhance the performance of NaLSuper for improving ssim. The smooth L1 loss demonstrates effectively enhance the performance of NaLSuper for improving psnr. The combination of SSIM and L1 loss, which quantifies the differences between output and ground truth features, effectively aids the model in accurately restoring image color, texture, and fine details.

V. CONCLUSION

In this paper, we introduce a Natural Language Supervision network (NaLSuper) designed to enhance images taken in low-light conditions. This network addresses several challenges simultaneously, including low contrast, insufficient lighting, noise, and color distortions. Firstly, we design a Textual

| LOSS | Metric | LOLv1 | LOLv2-real | LOLv2-syn |
|---------|--------------------|--------|------------|-----------|
| L1 | PSNR \uparrow | 22.84 | 19.43 | 23.83 |
| | SSIM \uparrow | 0.816 | 0.813 | 0.920 |
| | LPIPS \downarrow | 0.1114 | 0.1406 | 0.0509 |
| | MAE \downarrow | 0.0788 | 0.1352 | 0.0748 |
| SSIM | PSNR \uparrow | 20.87 | 19.29 | 23.35 |
| | SSIM \uparrow | 0.831 | 0.831 | 0.921 |
| | LPIPS \downarrow | 0.0952 | 0.1114 | 0.0599 |
| | MAE \downarrow | 0.1063 | 0.1422 | 0.0762 |
| L1+SSIM | PSNR \uparrow | 24.01 | 21.12 | 24.48 |
| | SSIM \uparrow | 0.863 | 0.846 | 0.930 |
| | LPIPS \downarrow | 0.0747 | 0.1001 | 0.0396 |
| | MAE \downarrow | 0.0756 | 0.1173 | 0.0718 |

TABLE V

PSNR, SSIM, LPIPS, AND MAE EVALUATION OF DIFFERENT LOSS FUNCTIONS IN LOLV1, LOLV2-REAL AND LOLV2-SYN DATASET

Guidance Conditioning Mechanism (TCM) to incorporating the connections between image regions and sentence words. In order to effectively identify and merge features from various levels of image and textual information, we design a Information Fusion Attention (IFA) module to do different levels of enhancement for different regions. Extensive experiments shows that NaLSuper effectively handles a wide range of low-light images and significantly surpasses current methods in performance.

REFERENCES

- [1] Rayan Al Sobhahi and Joe Tekli. Low-light homomorphic filtering network for integrating image enhancement and classification. *Signal Processing: Image Communication*, 100:116527, 2022.
- [2] Eric P Bennett and Leonard McMillan. Video enhancement using per-pixel virtual exposures. In *ACM SIGGRAPH 2005 Papers*, pages 845–852. 2005.
- [3] Chen Chen, Qifeng Chen, Jia Xu, and Vladlen Koltun. Learning to see in the dark. In *Proceedings of the IEEE conference on computer vision and pattern recognition*, pages 3291–3300, 2018.
- [4] Heng-Da Cheng and XJ Shi. A simple and effective histogram equalization approach to image enhancement. *Digital signal processing*, 14(2):158–170, 2004.
- [5] Jaemin Cho, Jie Lei, Hao Tan, and Mohit Bansal. Unifying vision-and-language tasks via text generation. In *International Conference on Machine Learning*, pages 1931–1942. PMLR, 2021.

- [6] Xuan Dong, Yi Pang, and Jiangtao Wen. Fast efficient algorithm for enhancement of low lighting video. In *ACM SIGGRAPH 2010 posters*, pages 1–1. 2010.
- [7] Benjamin Elizalde, Soham Deshmukh, Mahmoud Al Ismail, and Huaming Wang. Clap learning audio concepts from natural language supervision. In *ICASSP 2023-2023 IEEE International Conference on Acoustics, Speech and Signal Processing (ICASSP)*, pages 1–5. IEEE, 2023.
- [8] Xueyang Fu, Yinghao Liao, Delu Zeng, Yue Huang, Xiao-Ping Zhang, and Xinghao Ding. A probabilistic method for image enhancement with simultaneous illumination and reflectance estimation. *IEEE Transactions on Image Processing*, 24(12):4965–4977, 2015.
- [9] Xueyang Fu, Delu Zeng, Yue Huang, Yinghao Liao, Xinghao Ding, and John Paisley. A fusion-based enhancing method for weakly illuminated images. *Signal Processing*, 129:82–96, 2016.
- [10] Xueyang Fu, Delu Zeng, Yue Huang, Xiao-Ping Zhang, and Xinghao Ding. A weighted variational model for simultaneous reflectance and illumination estimation. In *Proceedings of the IEEE conference on computer vision and pattern recognition*, pages 2782–2790, 2016.
- [11] Xiuye Gu, Tsung-Yi Lin, Weicheng Kuo, and Yin Cui. Open-vocabulary object detection via vision and language knowledge distillation. *arXiv preprint arXiv:2104.13921*, 2021.
- [12] Chunle Guo, Chongyi Li, Jichang Guo, Chen Change Loy, Junhui Hou, Sam Kwong, and Runmin Cong. Zero-reference deep curve estimation for low-light image enhancement. In *Proceedings of the IEEE/CVF conference on computer vision and pattern recognition*, pages 1780–1789, 2020.
- [13] Xiaojie Guo, Yu Li, and Haibin Ling. Lime: Low-light image enhancement via illumination map estimation. *IEEE Transactions on image processing*, 26(2):982–993, 2016.
- [14] Shijie Hao, Xu Han, Yanrong Guo, Xin Xu, and Meng Wang. Low-light image enhancement with semi-decoupled decomposition. *IEEE transactions on multimedia*, 22(12):3025–3038, 2020.
- [15] Kaiming He, Jian Sun, and Xiaoou Tang. Single image haze removal using dark channel prior. *IEEE transactions on pattern analysis and machine intelligence*, 33(12):2341–2353, 2010.
- [16] Md Jahidul Islam, Chelsey Edge, Yuyang Xiao, Peigen Luo, Muntaqim Mehtaz, Christopher Morse, Sadman Sakib Enan, and Junaed Sattar. Semantic segmentation of underwater imagery: Dataset and benchmark. In *2020 IEEE/RSJ International Conference on Intelligent Robots and Systems (IROS)*, pages 1769–1776. IEEE, 2020.
- [17] Andrew Jaegle, Felix Gimeno, Andy Brock, Oriol Vinyals, Andrew Zisserman, and Joao Carreira. Perceiver: General perception with iterative attention. In *International conference on machine learning*, pages 4651–4664. PMLR, 2021.
- [18] Chao Jia, Yinfei Yang, Ye Xia, Yi-Ting Chen, Zarana Parekh, Hieu Pham, Quoc Le, Yun-Hsuan Sung, Zhen Li, and Tom Duerig. Scaling up visual and vision-language representation learning with noisy text supervision. In *International conference on machine learning*, pages 4904–4916. PMLR, 2021.
- [19] Yifan Jiang, Xinyu Gong, Ding Liu, Yu Cheng, Chen Fang, Xiaohui Shen, Jianchao Yang, Pan Zhou, and Zhangyang Wang. Enlightengan: Deep light enhancement without paired supervision. *IEEE transactions on image processing*, 30:2340–2349, 2021.
- [20] Woojeong Jin, Yu Cheng, Yelong Shen, Weizhu Chen, and Xiang Ren. A good prompt is worth millions of parameters: Low-resource prompt-based learning for vision-language models. *arXiv preprint arXiv:2110.08484*, 2021.
- [21] Daniel J Jobson, Zia-ur Rahman, and Glenn A Woodell. A multiscale retinex for bridging the gap between color images and the human observation of scenes. *IEEE Transactions on Image processing*, 6(7):965–976, 1997.
- [22] Chen Ju, Tengda Han, Kunhao Zheng, Ya Zhang, and Weidi Xie. Prompting visual-language models for efficient video understanding. In *European Conference on Computer Vision*, pages 105–124. Springer, 2022.
- [23] Yeong-Taeg Kim. Contrast enhancement using brightness preserving bi-histogram equalization. *IEEE transactions on Consumer Electronics*, 43(1):1–8, 1997.
- [24] Rushi Lan, Long Sun, Zhenbing Liu, Huimin Lu, Cheng Pang, and Xiaonan Luo. Madnet: a fast and lightweight network for single-image super resolution. *IEEE transactions on cybernetics*, 51(3):1443–1453, 2020.
- [25] Chongyi Li, Chunle Guo, and Chen Change Loy. Learning to enhance low-light image via zero-reference deep curve estimation. *IEEE Transactions on Pattern Analysis and Machine Intelligence*, 44(8):4225–4238, 2021.
- [26] Chongyi Li, Jichang Guo, Fatih Porikli, and Yanwei Pang. Lightnetnet: A convolutional neural network for weakly illuminated image enhancement. *Pattern recognition letters*, 104:15–22, 2018.
- [27] Jinjiang Li, Xiaomei Feng, and Zhen Hua. Low-light image enhancement via progressive-recursive network. *IEEE Transactions on Circuits and Systems for Video Technology*, 31(11):4227–4240, 2021.
- [28] Seokjae Lim and Wonjun Kim. Dslr: Deep stacked laplacian restorer for low-light image enhancement. *IEEE Transactions on Multimedia*, 23:4272–4284, 2020.
- [29] Risheng Liu, Long Ma, Jiaao Zhang, Xin Fan, and Zhongxuan Luo. Retinex-inspired unrolling with cooperative prior architecture search for low-light image enhancement. In *Proceedings of the IEEE/CVF Conference on Computer Vision and Pattern Recognition*, pages 10561–10570, 2021.
- [30] Wei Liu, Dragomir Anguelov, Dumitru Erhan, Christian Szegedy, Scott Reed, Cheng-Yang Fu, and Alexander C Berg. Ssd: Single shot multibox detector. In *Computer Vision—ECCV 2016: 14th European Conference, Amsterdam, The Netherlands, October 11–14, 2016, Proceedings, Part I 14*, pages 21–37. Springer, 2016.
- [31] Kin Gwn Lore, Adedotun Akintayo, and Soumik Sarkar. Llnet: A deep autoencoder approach to natural low-light image enhancement. *Pattern Recognition*, 61:650–662, 2017.
- [32] Long Ma, Risheng Liu, Jiaao Zhang, Xin Fan, and Zhongxuan Luo. Learning deep context-sensitive decomposition for low-light image enhancement. *IEEE Transactions on Neural Networks and Learning Systems*, 33(10):5666–5680, 2021.
- [33] Stephen M Pizer. Contrast-limited adaptive histogram equalization: Speed and effectiveness stephen m. pizer, r. eugene johnston, james p. ericksen, bonnie c. yankaskas, keith e. muller medical image display research group. In *Proceedings of the first conference on visualization in biomedical computing, Atlanta, Georgia*, volume 337, page 1, 1990.
- [34] Xu Qin, Zhilin Wang, Yuanhao Bai, Xiaodong Xie, and Huizhu Jia. Ffa-net: Feature fusion attention network for single image dehazing. In *Proceedings of the AAAI conference on artificial intelligence*, volume 34, pages 11908–11915, 2020.
- [35] Alec Radford, Jong Wook Kim, Chris Hallacy, Aditya Ramesh, Gabriel Goh, Sandhini Agarwal, Girish Sastry, Amanda Askell, Pamela Mishkin, Jack Clark, et al. Learning transferable visual models from natural language supervision. In *International conference on machine learning*, pages 8748–8763. PMLR, 2021.
- [36] Yongming Rao, Wenliang Zhao, Guangyi Chen, Yansong Tang, Zheng Zhu, Guan Huang, Jie Zhou, and Jiwen Lu. Densclip: Language-guided dense prediction with context-aware prompting. In *Proceedings of the IEEE/CVF conference on computer vision and pattern recognition*, pages 18082–18091, 2022.
- [37] Wenqi Ren, Sifei Liu, Lin Ma, Qianqian Xu, Xiangyu Xu, Xiaochun Cao, Junping Du, and Ming-Hsuan Yang. Low-light image enhancement via a deep hybrid network. *IEEE Transactions on Image Processing*, 28(9):4364–4375, 2019.
- [38] Sheng Shen, Liunian Harold Li, Hao Tan, Mohit Bansal, Anna Rohrbach, Kai-Wei Chang, Zhewei Yao, and Kurt Keutzer. How much can clip benefit vision-and-language tasks? *arXiv preprint arXiv:2107.06383*, 2021.
- [39] Pengfei Shi, Xiwang Xu, Xinnan Fan, Xudong Yang, and Yuanxue Xin. Ll-unet++: Unet++ based nested skip connections network for low-light image enhancement. *IEEE Transactions on Computational Imaging*, 2024.
- [40] Yanan Sun, Bing Xue, Mengjie Zhang, Gary G Yen, and Jiancheng Lv. Automatically designing cnn architectures using the genetic algorithm for image classification. *IEEE transactions on cybernetics*, 50(9):3840–3854, 2020.
- [41] Ashish Vaswani, Noam Shazeer, Niki Parmar, Jakob Uszkoreit, Llion Jones, Aidan N Gomez, Łukasz Kaiser, and Illia Polosukhin. Attention is all you need. *Advances in neural information processing systems*, 30, 2017.
- [42] Li-Wen Wang, Zhi-Song Liu, Wan-Chi Siu, and Daniel PK Lun. Lightening network for low-light image enhancement. *IEEE Transactions on Image Processing*, 29:7984–7996, 2020.
- [43] Mengmeng Wang, Jiazheng Xing, and Yong Liu. Actionclip: A new paradigm for video action recognition. *arXiv preprint arXiv:2109.08472*, 2021.
- [44] Shuhang Wang, Jin Zheng, Hai-Miao Hu, and Bo Li. Naturalness preserved enhancement algorithm for non-uniform illumination images. *IEEE transactions on image processing*, 22(9):3538–3548, 2013.
- [45] Suchen Wang, Yueqi Duan, Henghui Ding, Yap-Peng Tan, Kim-Hui Yap, and Junsong Yuan. Learning transferable human-object interaction detector with natural language supervision. In *Proceedings of the*

- IEEE/CVF Conference on Computer Vision and Pattern Recognition*, pages 939–948, 2022.
- [46] Tao Wang, Kaihao Zhang, Tianrun Shen, Wenhan Luo, Bjorn Stenger, and Tong Lu. Ultra-high-definition low-light image enhancement: A benchmark and transformer-based method. In *Proceedings of the AAAI Conference on Artificial Intelligence*, volume 37, pages 2654–2662, 2023.
- [47] Yu Wang, Qian Chen, and Baomin Zhang. Image enhancement based on equal area dualistic sub-image histogram equalization method. *IEEE transactions on Consumer Electronics*, 45(1):68–75, 1999.
- [48] Zhendong Wang, Xiaodong Cun, Jianmin Bao, Wengang Zhou, Jianzhuang Liu, and Houqiang Li. Uformer: A general u-shaped transformer for image restoration. In *Proceedings of the IEEE/CVF conference on computer vision and pattern recognition*, pages 17683–17693, 2022.
- [49] Zhou Wang, Alan C Bovik, Hamid R Sheikh, and Eero P Simoncelli. Image quality assessment: from error visibility to structural similarity. *IEEE transactions on image processing*, 13(4):600–612, 2004.
- [50] Chen Wei, Wenjing Wang, Wenhan Yang, and Jiaying Liu. Deep retinex decomposition for low-light enhancement. *arXiv preprint arXiv:1808.04560*, 2018.
- [51] Xi Wei, Tianzhu Zhang, Yan Li, Yongdong Zhang, and Feng Wu. Multi-modality cross attention network for image and sentence matching. In *Proceedings of the IEEE/CVF conference on computer vision and pattern recognition*, pages 10941–10950, 2020.
- [52] Wenhui Wu, Jian Weng, Pingping Zhang, Xu Wang, Wenhan Yang, and Jianmin Jiang. Uretinex-net: Retinex-based deep unfolding network for low-light image enhancement. In *Proceedings of the IEEE/CVF conference on computer vision and pattern recognition*, pages 5901–5910, 2022.
- [53] Ke Xu, Xin Yang, Baocai Yin, and Rynson WH Lau. Learning to restore low-light images via decomposition-and-enhancement. In *Proceedings of the IEEE/CVF conference on computer vision and pattern recognition*, pages 2281–2290, 2020.
- [54] Xiaogang Xu, Ruixing Wang, Chi-Wing Fu, and Jiaya Jia. Snr-aware low-light image enhancement. In *Proceedings of the IEEE/CVF Conference on Computer Vision and Pattern Recognition*, pages 17714–17724, 2022.
- [55] Wenhan Yang, Shiqi Wang, Yuming Fang, Yue Wang, and Jiaying Liu. From fidelity to perceptual quality: A semi-supervised approach for low-light image enhancement. In *Proceedings of the IEEE/CVF conference on computer vision and pattern recognition*, pages 3063–3072, 2020.
- [56] Zhenqiang Ying, Ge Li, and Wen Gao. A bio-inspired multi-exposure fusion framework for low-light image enhancement. *arXiv preprint arXiv:1711.00591*, 2017.
- [57] Syed Waqas Zamir, Aditya Arora, Salman Khan, Munawar Hayat, Fahad Shahbaz Khan, and Ming-Hsuan Yang. Restormer: Efficient transformer for high-resolution image restoration. In *Proceedings of the IEEE/CVF conference on computer vision and pattern recognition*, pages 5728–5739, 2022.
- [58] Syed Waqas Zamir, Aditya Arora, Salman Khan, Munawar Hayat, Fahad Shahbaz Khan, Ming-Hsuan Yang, and Ling Shao. Learning enriched features for real image restoration and enhancement. In *Computer Vision—ECCV 2020: 16th European Conference, Glasgow, UK, August 23–28, 2020, Proceedings, Part XXV 16*, pages 492–511. Springer, 2020.
- [59] Yonghua Zhang, Xiaojie Guo, Jiayi Ma, Wei Liu, and Jiawan Zhang. Beyond brightening low-light images. *International Journal of Computer Vision*, 129:1013–1037, 2021.
- [60] Yonghua Zhang, Jiawan Zhang, and Xiaojie Guo. Kindling the darkness: A practical low-light image enhancer. In *Proceedings of the 27th ACM international conference on multimedia*, pages 1632–1640, 2019.
- [61] Zhao Zhang, Huan Zheng, Richang Hong, Mingliang Xu, Shuicheng Yan, and Meng Wang. Deep color consistent network for low-light image enhancement. In *Proceedings of the IEEE/CVF conference on computer vision and pattern recognition*, pages 1899–1908, 2022.
- [62] Zunjin Zhao, Bangshu Xiong, Lei Wang, Qiaofeng Ou, Lei Yu, and Fa Kuang. Retinexdip: A unified deep framework for low-light image enhancement. *IEEE Transactions on Circuits and Systems for Video Technology*, 32(3):1076–1088, 2021.
- [63] Yiwu Zhong, Jing Shi, Jianwei Yang, Chenliang Xu, and Yin Li. Learning to generate scene graph from natural language supervision. In *Proceedings of the IEEE/CVF International Conference on Computer Vision*, pages 1823–1834, 2021.
- [64] Kaiyang Zhou, Jingkang Yang, Chen Change Loy, and Ziwei Liu. Learning to prompt for vision-language models. *International Journal of Computer Vision*, 130(9):2337–2348, 2022.
- [65] Lingyu Zhu, Wenhan Yang, Baoliang Chen, Fangbo Lu, and Shiqi Wang. Enlightening low-light images with dynamic guidance for context enrichment. *IEEE Transactions on Circuits and Systems for Video Technology*, 32(8):5068–5079, 2022.